Plant-inspired soft actuators powered by water

Beomjune Shin,† Sohyun Jung,† Munkyeong Choi, Keunhwan Park,* and Ho-Young Kim*

Unlike animals, plants lack motion-generating systems such as a central nervous system or muscles, but they have successfully developed mechanisms to sense and respond to environmental changes, ensuring their survival. Most of their movements rely on the movement of water into and out of their cells or tissues, which are intrinsically soft and porous. Understanding and harnessing these natural processes can lead to the development of environmentally friendly and biocompatible soft actuator systems. This article explains the strategies employed by plants to generate movement through water transportation, categorizing them into osmosis-driven and hygroscopic swelling-driven mechanisms. Additionally, we discuss the latest trends in soft actuators that replicate plant water-utilizing movements, suggest directions for further development, and provide a review of practical applications.

Introduction

Plant biomechanics have become an exciting avenue for technological advances, especially in the design of soft actuators.[1–6] Physicochemical understanding of plant motion mechanisms allows for a unique perspective in creating devices that mimic dynamic and adaptive behaviors of plants that have survived for billions of years. These innovations can play significant roles in fields, such as robotics,[7–10] biomedical devices,[11,12] and stimuli-responsive materials.[13,14]

Unlike animals, plants lead a sedentary lifestyle due to their roots, which absorb water and essential inorganic substances from the soil for survival.[15–17] While these roots enable the absorption of vital resources, they also limit the mobility of plants. To adapt to this lifestyle, plants have evolved strategies to mitigate rather than evade. Specifically, plants lack the centralized systems found in animals, which oversee the overall conditions of the individual.[18] For example, plants do not have supplementary organs, such as the nervous and circulatory systems. They also lack muscles, which severely limits their ability to generate movement. This simplicity increases their survival probability, even when parts of them are severed by predators or natural disasters, and minimizes the cost of repairing or regenerating lost organs.

Interestingly, despite their lack of a central nervous system and muscles, plants can sense and react to environmental changes in ways that promote their survival. They have evolved ingenious mechanisms for perceiving threats and responding so as to ensure their survival and reproduction.[19,20] Understanding how plants achieve this, despite their seemingly simple structure, has been one of major thrusts in recent advancements in plant biomechanics research.[21,22] This article will introduce recent important findings in this respect, focusing on how plants perceive and respond to environmental changes without a central nervous system or the ability to move in the way animals do.

Our exploration will delve into the two main ways plants harness water to generate motion: osmosis and hygroexpansion. These mechanisms, although reliant on different processes, demonstrate the remarkable power and potential of water as a driving force for motility. We will also discuss the

Beomjune Shin, George W. Woodruff School of Mechanical Engineering, Georgia Institute of Technology, Atlanta, USA; sbj0602@gmail.com
Sohyun Jung, Department of Mechanical Engineering, Seoul National University, Seoul, Korea; sohyun153@snu.ac.kr
Munkyeong Choi, Department of Mechanical Engineering, Seoul National University, Seoul, Korea; hungry604@snu.ac.kr
Keunhwan Park, Department of Mechanical Engineering, Gachon University, Seongnam, Korea; kpark@gachon.ac.kr
Ho-Young Kim, Department of Mechanical Engineering, Seoul National University, Seoul, Korea; Institute of Advanced Machines and Design, Seoul National University, Seoul, Korea; hyk@snu.ac.kr
*Corresponding author
†Beomjune Shin and Sohyun Jung have contributed equally to this work.
doi:10.1557/s43577-024-00663-3

latest development of artificial actuators inspired by these plants. By understanding and harnessing these processes, we can open the door to a new era of soft actuators that are efficient, adaptable, environmentally friendly, biocompatible, and scalable. This article will also serve as a foundation for further R&D in plant-inspired soft robotics.

Osmotic actuation

Osmosis in plant physiology

Osmosis, a process driven by solute concentration gradients across semipermeable cellular membranes, enables water molecules to move from regions of lower to higher solute concentration. This movement is induced by a chemical potential difference or osmotic pressure. In plant cells, this process manifests itself prominently through the actions of vacuoles. These large organelles contain a solution of water and various dissolved substances, such as nutrients and waste products, and expand by absorbing water through osmosis. The resultant expansion works synergistically with the rigid cell wall, unique to plant cells (**Figure 1**a), to generate high internal hydrostatic pressure, known as turgor pressure.[23] Turgor pressure is integral to several functions, including nutrient transport,[24,25] structural support,[26–29] and particularly, the facilitation of osmotic movements.

Motor cells in plants are specialized to undergo changes in their osmotic pressure, which leads to differences in turgor pressure. The changes in turgor pressure directly impact the cell's volume and length, causing physical movements or displacements within the plant. When the turgor pressure of these motor cells is altered, it can influence the surrounding nonmotor cells within the same plant organ. This causes the organ itself to bend. This process, where changes in osmotic pressure direct plant movements, plays a critical role in many different types of plant movement. These include the opening and closing of stomata, a process crucial for gas exchange and leaf transpiration (Figure 1b),[30–32] and the motion of leaves or flowers by pulvinus motor cells (Figure 1c).[33,34] In addition, this mechanism facilitates specialized movements such as leaf curling in Drosera (Figure 1d),[35–37] and Mimosa leaf movements (Figure 1e).[38–40] The operation of the Venus flytrap (Figure 1f),[41–45] and movements of stamens and stigmas in various flowers,[46] as well as the opening and closing of Utricularia's bladder trapdoor,[47] are also enabled by this osmotic pressure-driven mechanism.

Principles of osmotic actuation and their application in soft actuators

Osmosis, essential for plant water transport, offers a promising actuation mechanism for high-performance soft actuators. Osmotic actuation, governed by osmotic pressure π as described by the van't Hoff Law ($\pi = cRT$), with R and T, respectively, being the universal gas constant (8.32 J K^{-1} mol^{-1}) and the temperature,[48,49] predominantly depends on solute concentration, c. Consequently, actuation can be modulated by altering the quantity of activated solute molecules. By adding common salts such as NaCl, KCl, or NH_4Cl with a molar solubility of ~1000 mol m^{-3} in pure water under ambient conditions,[50] osmotic pressure of ~1 MPa can be achieved. This surpasses pressures in standard mechanical systems, such as car tires (0.14–0.35 MPa) and residential water supplies (≈0.3 MPa), highlighting the potential of osmotic actuation in soft actuators (Figure 1g). Plant osmotic pressure typically ranges from 0.1 to 6 MPa (Figure 1g). Leaf and root cells register osmotic pressures of 0.25–0.3 MPa[51,52] and up to 0.65 MPa,[53,54] respectively. Movement-related cells such as stomata's guard cells and pulvini's extensor and flexor cells exhibit pressures of 4 MPa[55] and 1 MPa,[56,57] respectively. Notably, *Phakopsora pachyrhizi* appressoria recorded pressures as high as 5–6 MPa.[58]

Turning to osmotic actuation speed, it is determined by the osmotic water flux, represented by $j = K(\Delta p - \sigma\Delta\pi)$,[59,60] where K is the membrane's hydraulic conductivity, Δp is the hydrostatic pressure difference, and σ is the solute's reflection ($0 \leq \sigma \leq 1$). In an osmotic system encapsulated by an ideal semipermeable membrane and submerged in a liquid under atmospheric conditions, the water flux across the membrane, j simplifies to $K\Delta\pi$. The response time, τ for osmotic actuation is scaled as $\delta/(K\Delta\pi)$, where δ is the plant cell size. Plant cells (~10 μm) display membrane conductivities of $10^{-13} < K < 10^{-11}$ m s^{-1} Pa^{-1}.[61] Considering $\Delta\pi \sim 1$ MPa and $K \sim 10^{-12}$ m s^{-1} Pa^{-1}, these cells yield $\tau \sim 1$ s.[61] Some plant cells expedite actuation by increasing osmotic pressure via ion transport, with ion flux rates ranging from $10^{-7} < j_s^* < 10^{-6}$ mol m^{-2} s^{-1},[32,40] thereby augmenting osmotic pressure by ~10−100 Pa s^{-1}. Thus, osmotic actuation in plant cells shows impressive energy storage and speed, shedding light on potential high-performance soft actuator development.

To incorporate osmotic principles into soft actuator design, we need to separate ionic solutions of different concentrations while facilitating water movement and inhibiting ion migration (**Figure 2**a). Plants achieve this effectively with semipermeable membranes, and many osmotic actuators have emulated this strategy.[7,62–65] However, artificial systems face limitations, such as the need for external fluid transfer to alter solute concentration for tunable actuation and the complex task of creating a sealed, leak-proof system (Figure 2b). A recent osmotic actuator attempts to address these issues by regulating osmotic actuation via the reversible adjustment of activated solute molecules, using flexible porous carbon electrodes and electric forces (Figure 2c).[7] This led to reversible stiffening and rotation in soft robots. However, the complexity of fabrication remains challenging, hindering the scale-down of systems crucial for high actuation speeds.

Hydrogels, intrinsically capable of leveraging osmosis, have significant advantages in addressing these fabrication complexities. In the subsequent sections, we will explore hydrogel actuators, focusing on understanding how they leverage osmosis, the methods they employ to generate

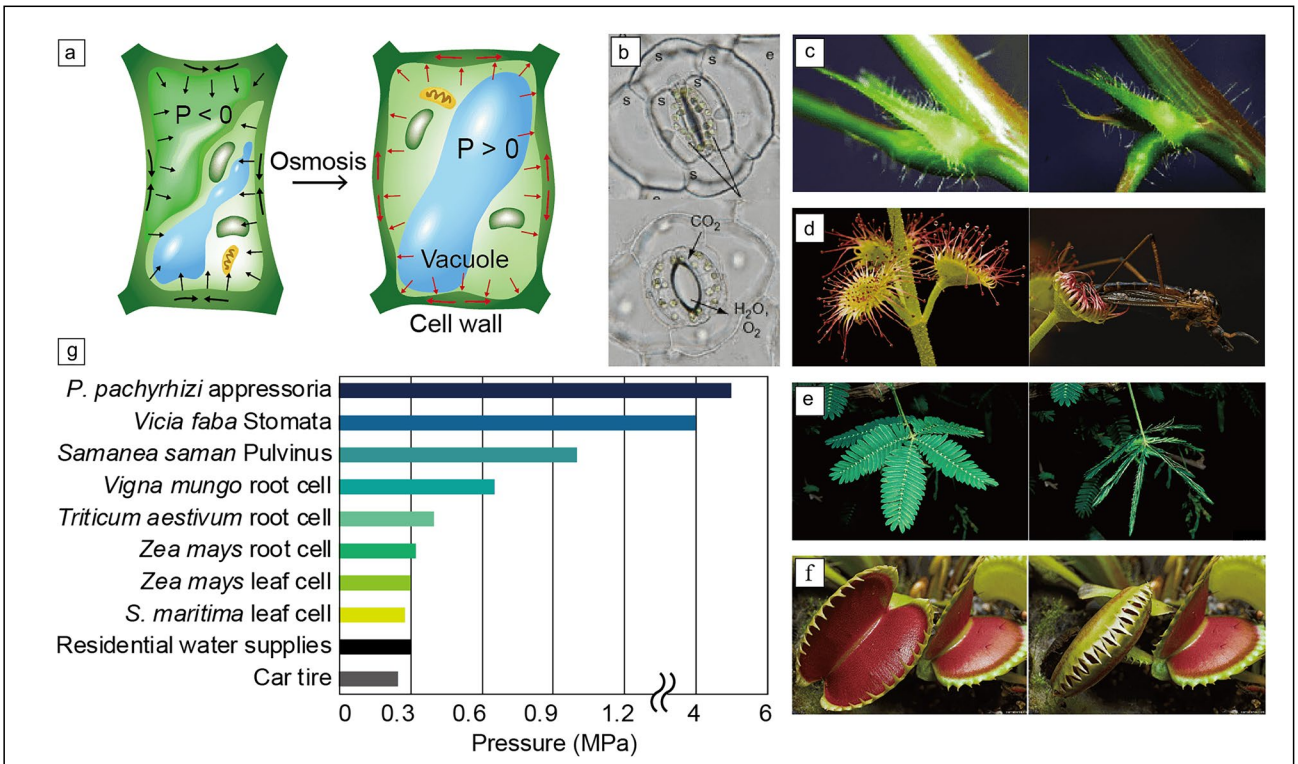

Figure 1. (a) Development of turgor pressure, ***p***, through osmosis in an isolated plant cell with a rigid structural component, the cell wall. (b) Closed and open stomata from the epidermis of *Commelina benghalensis*. Adapted with permission from Reference 31. © 2011 Elsevier. (c) Main pulvinus of *Mimosa pudica* showing the changes from its open state to closed state after mechanical stimulation. Adapted with permission from Reference 33. © 2000 Springer Nature. (d) *Drosera stolonifera* with open leaves and leaves folded to capture prey. (e) *Mimosa pudica* before and after touch stimulation. (f) Venus flytrap (*Dionaea muscipula*) with its trap in open and closed states. (d–f) Photos by B.A. Rice (2018). The Carnivorous Plant FAQ v.12. https://www.sarracenia.com/faq.html. (g) Comparison of hydrostatic pressures of plant cells and common mechanical systems, such as car tires and residential water supplies.

actuation, and a brief analysis of the actuation speed and power output characteristics.

Hydrogel actuators

Hydrogels are cross-linked, hydrophilic polymer chains that function as solutes, creating an intrinsic osmotic pressure difference between the materials interior and exterior. As illustrated in **Figure 3**a, hydrogels can absorb water and expand their volume due to this osmotic pressure. Beyond this osmotic expansion capability, hydrogels also exhibit tunable mechanical properties, biocompatibility, transparency, and sensitivity to various external stimuli. Combined with their ease of fabrication, these properties make hydrogels appealing for efficient and high-performance soft actuators.

The performance of hydrogel actuators hinges significantly on the hydrogel's swelling behavior, which is represented by the swelling ratio reflecting the fractional volume increase due to water absorption. This behavior is primarily governed by such factors as osmotic pressure, electrical potential, and hydrogel stress. Here, the osmotic pressure and electrical potential are highly related to the surrounding environmental conditions, including both chemical (pH, ions, and solvent composition) and physical (temperature, light, mechanical stress, and electric field) stimuli.[66,67] Microstructural characteristics of hydrogels, such as the type and concentration of monomers, the type and density of cross-links, and porosity, significantly impact the hydrogel stress and thus are also crucial determinants of their swelling behavior.[68,69]

External stimulus-driven actuation

The behavior of hydrogel actuators can be modulated by various external stimuli, including water,[70,71] pH,[72,73] temperature,[74] light,[75,76] electric fields,[77] and enzymes[78] allowing for the creation of a diverse range of stimuli-responsive systems. The most intuitive, hydro-responsive hydrogel actuator was presented by Yang et al.[70] wherein the hydrogel was localized at the system's tip. The localized swelling and shape changes upon contact with water led to application in microneedles for tissue mechanical interlocking (Figure 3b).

Using the pH-responsive swelling property of hydrogels, Beebe et al.[72] developed autonomous flow-regulating valves in microchannels that react adaptively to environmental conditions. Similarly, Shastri et al.[73] developed hydrogel actuators by embedding polymeric micro-fins within pH-responsive hydrogels. These actuators mimic muscle action through pH-triggered swelling and shrinking, resulting in reversible micro-fin bending. When paired with a molecule-specific binding element on

the fin tips, these actuators efficiently capture, transport, and separate biomolecules within a microfluidic system (Figure 3c).

Temperature-responsive hydrogel actuators, paired with the tunable swelling ratio and superior transparency of hydrogels, were used in a liquid lens system. This system focuses autonomously by adjusting droplet shape and focal length in response to the temperature (Figure 3d).[74]

Furthermore, external stimuli such as light, electric fields, and enzymes can modulate the hydrogel's microstructural parameters. One example of such manipulations is controlling the local degree of cross-linking, thereby achieving spatially patterned swelling via UV exposure (Figure 3e).[75,76] Another approach, termed "ionoprinting," promotes localized cation binding within anionic hydrogels via a controlled electrical potential to a patterned anode. This method modulates the local swelling ratio via the regulated imprinting depth, leading to controlled curvature (Figure 3f).[77] Further, in hybrid gels with both enzyme-responsive and nonresponsive polymer chains, specific enzymes can selectively degrade the responsive chains, thereby reducing stiffness and enabling shape transformation.[78] These advancements offer a wider potential for complex, precise movements in soft robotics, including elongation, bending, folding, twisting, and locomotion.

Microelement-embedded actuation

Alternative methods to achieve precise and complex movements in hydrogel actuators involve the use of embedded microelements. A notable application of this method is seen in the use of microelements serving as directional constraints. In one such implementation, stiff cellulose fibrils were embedded and aligned within hydrogels during the 3D printing process (Figure 3g). This resulted in localized anisotropy, enabling the actuator to morph into predefined complex 3D structures upon water immersion.[79]

In addition, microelements can serve as actuation drivers. Kim et al.[80] used co-facially oriented electrolyte nanosheets as actuation drivers within a hydrogel actuator. The notable aspect of this mechanism was the temperature-modulated electrostatic interactions between nanosheets, causing significant elongation and contraction of the hydrogel (Figure 3h). Similarly, Liu et al.[81] introduced small superabsorbent particles into a hydrogel shell membrane to create a device with a high swelling ratio and long-term robustness. The device, designed to be ingested such as a regular-sized pill, rapidly expands into a large, soft sphere upon exposure to water and maintains its integrity in the stomach for up to a month despite repeated mechanical stresses.

Actuation speed and forces in hydrogel actuators

Actuation speed is a critical attribute of actuators. For hydrogel actuators, the actuation speed is primarily determined by the rate of swelling, which is linked to the actuator size and hydrogel's permeability—a property influenced by its microstructure, including porosity, individual pore size, and pore geometry. Several strategies have been proposed and implemented to enhance the actuation speed of these actuators. A straightforward and common method is scaling down to minimize the effective diffusion length. Techniques such as the fragmentation of a large hydrogel component into numerous small particles,[81] or size reduction of the actuator[72] were employed to this end. Another speed enhancement strategy focuses on modifying the gel's microstructure. Yoshida et al.,[82] for example, succeeded in inducing rapid deswelling of a hydrogel by tailoring the gel's architecture at the molecular

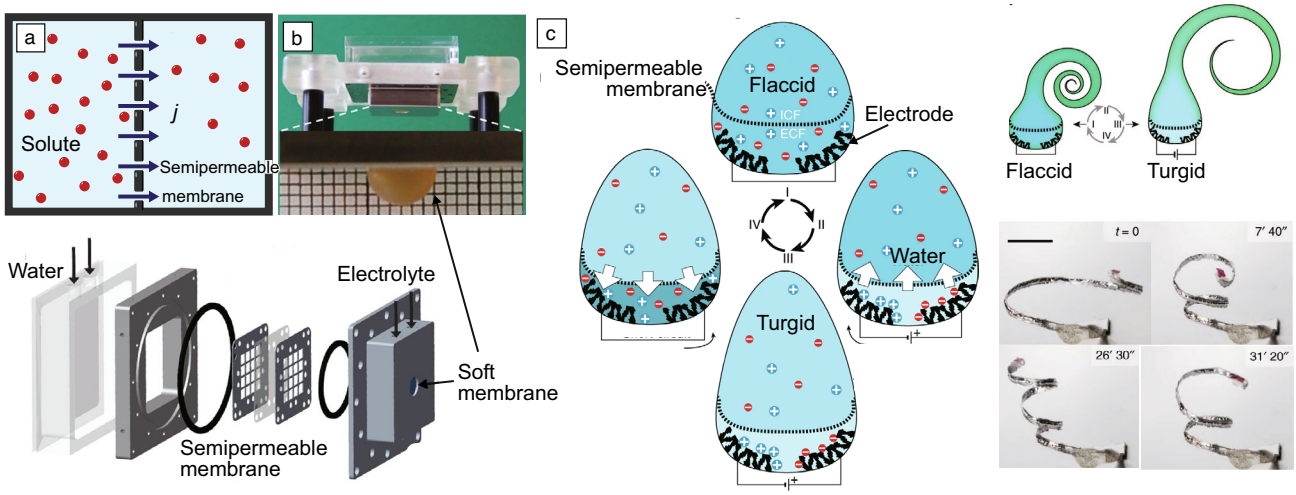

Figure 2. (a) Osmotic flow with the flux *j* across the semipermeable membrane. (b) A soft actuator design comprising two chambers, each with different ion concentrations, separated by a semipermeable membrane. The hydrostatic pressure driven by osmosis results in deformation of soft membrane. Adapted with permission from Reference 62. © 2014 Sinibaldi et al. (c) A soft osmotic actuator realizing tunable actuation by regulating osmotic pressure through the reversible adjustment of activated solute molecules using flexible porous carbon electrodes and electric forces. Adapted with permission from Reference 7. © 2019 Springer Nature.

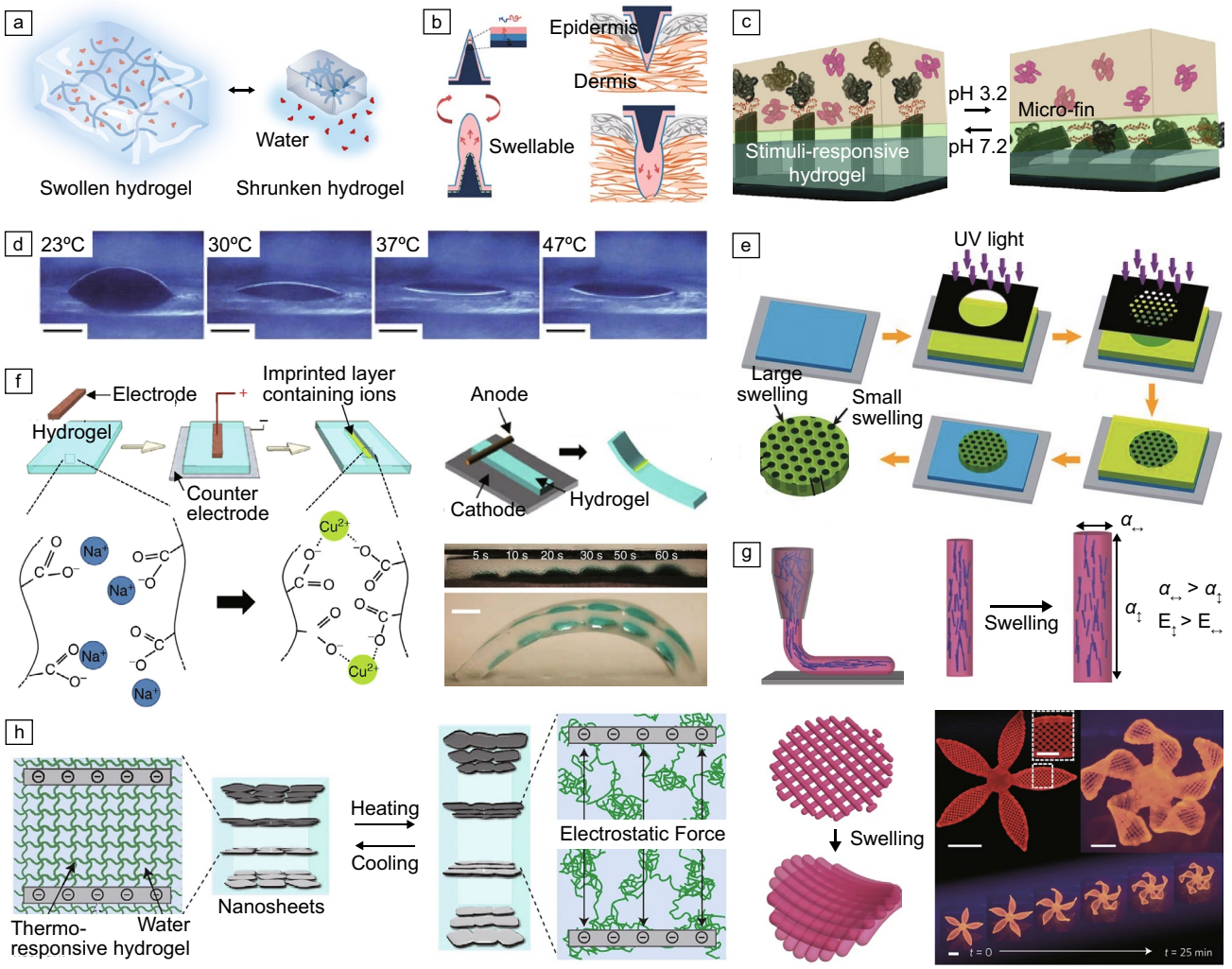

Figure 3. (a) Hydrogel, composed of 3D hydrophilic polymer networks, absorb water by osmosis and swell. (b) A hydro-responsive hydrogel actuator developed by Yang et al.[70] Adapted with permission from Reference 70. © 2013 Springer Nature. (c) A pH-responsive hydrogel actuator having polymeric micro-fins embedded within the hydrogels. Adapted with permission from Reference 73. © 2015 Springer Nature. (d) Liquid lens system based on temperature-responsive hydrogel actuators. (Scale bar: 1 mm) Adapted with permission from Reference 74. © 2006 Springer Nature. (e) Halftone gel lithography process using a photo-cross-linkable hydrogel. Spatially patterned swelling achieved through local UV exposure. Adapted with permission from Reference 76. © 2012 AAAS. (f) "Ionoprinting" technique that achieves controlled swelling ratio by imprinting ions via electric fields. (Scale bar: 3 mm) Adapted with permission from Reference 77. © 2013 Springer Nature. (g) Embedding of stiff cellulose fibrils within hydrogels for localized anisotropy. The cellulose fibrils are aligned during the printing process. (Scale bar: 5 mm, inset: 2.5 mm) Adapted with permission from Reference 79. © 2016 Springer Nature. (h) Thermoresponsive hydrogel actuator with a layered structure of unilamellar titanate (IV) nanosheets. Significant elongation and contraction of a hydrogel actuator is obtained using co-facially oriented electrolyte nanosheets. Adapted with permission from Reference 80. © 2015 Springer Nature.

level. Moreover, the actuation speed can be increased by enhancing imbibition rate through external stimuli, as Na et al.[3] demonstrated by combining electro-osmosis with osmotic flow to achieve rapid movement in a polyelectrolyte hydrogel actuator. Alternatively, the actuation speed can be improved by utilizing forces induced by the embedded materials. A notable example of this approach was shown by Kim et al.[80] with nanosheets as actuation drivers in a hydrogel actuator, as previously mentioned. Furthermore, increasing actuation speed in hydrogels can be achieved by embedding structural instability through mechanical property gradients. Fan et al.[83] demonstrate this using hydrogel sheets with dual-gradient structures, specifically gradients in chain and cross-linking density along their thickness. This design enables the accumulation of elastic energy by converting prestored energy, facilitating fast motion (under 1 s) via its immediate release.

A prevalent challenge in the development of hydrogel actuators is the tradeoff between actuation speed and force. Typically, a higher actuation force requires a larger hydrogel, which in turn, results in a longer response time.[84] As a result, hydrogel actuators have often been restricted by either low actuation speeds (with response times ranging from 10 min to

10 h) or low actuation forces (ranging from 1 to 10 mN).[80,85,86] However, recent advancements have started to overcome these limitations. A significant breakthrough was made by Na et al.,[3] which was inspired by plant cells to design a rapid and strong hydrogel actuator wrapped by a stiff membrane emulating cell walls capable of both rapid and strong actuation (**Figure 4**a).

Limitations and perspective of osmotic actuators

Osmosis in plants has provided an inspiring model for the design of soft actuators, a concept traditionally realized via semipermeable membranes paired with ionic solutions. Despite the scalability and versatility of these actuators, they are beset with intricate fabrication challenges, largely due to the complexity of artificially replicating natural osmotic mechanisms. Recently, hydrogels have emerged as a convenient and robust material for osmotic actuators owing to their straightforward fabrication process and inherent osmotic pressure generation capabilities, thereby significantly simplifying the fabrication complexities associated with traditional actuator designs.

Although hydrogels present promising advantages for osmotic actuators, their durability remains a paramount concern. For hydrogel actuators to function effectively under repetitive or high-stress operations, the hydrogels must possess both toughness and mechanical strength. However, conventional hydrogels often exhibit inherent weaknesses in their mechanical properties due to factors, such as low polymer density, an inhomogeneous network, and inadequate interpolymer chain friction. This often results in a brittle and fragile structure when subjected to mechanical loading, primarily because of a lack of an effective energy dissipation mechanism. Numerous attempts have been made to enhance mechanical properties by strategically redesigning the network structure, yet concurrently improving both hydrogel strength and toughness remains an ongoing challenge. In addition, even after the successful development of strong and tough hydrogels, fabricating these hydrogels into sophisticated 3D structural elements is needed for the commercialization of highly advanced hydrogel actuators.

Another challenge lies in achieving the molecular-scale dimensions essential for bio-related applications. Given the limitations of current hydrogel fabrication techniques, achieving these extremely small dimensions remains an elusive goal, calling for alternative approaches. For these scales, liposome-based actuators may offer potential solutions. Liposomes, spherical vesicles composed of phospholipid bilayers, have the potential for osmotic actuation due to their core–shell structure separated by a semipermeable layer (Figure 4b).[87–89] A handful of examples of these actuators exist, including the work by Shoji et al.[89] They demonstrated movement of liposome-inspired actuators by creating a solute concentration difference at the front and back of the actuators in a microchannel (Figure 4c), a setup akin to the "osmotic engine model" of cellular migration.[90]

As osmosis is fundamentally a specialized form of diffusion, it experiences a decline in efficiency as the scale increases. To overcome this physical constraint, some plants such as Venus flytrap[41] have evolved to wisely combine

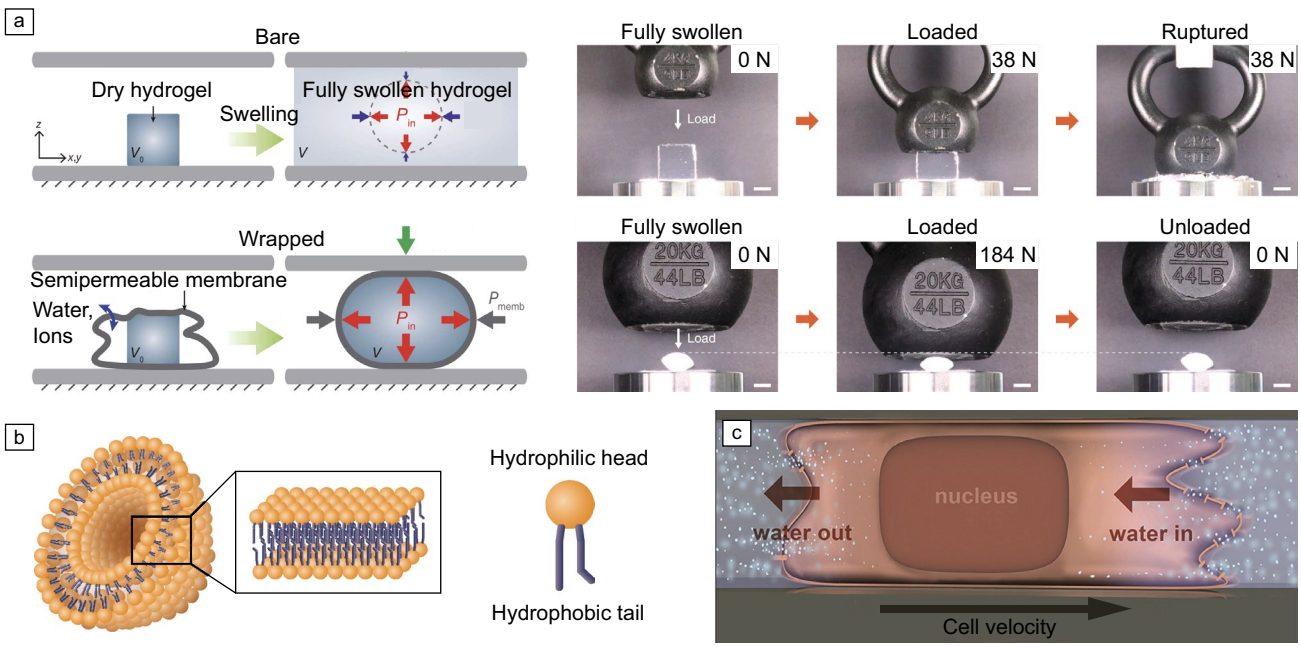

Figure 4. (a) A hydrogel actuator with hydrogel enclosed by a rigid semipermeable membrane, inspired by plant cells. This design enables both rapid and strong actuation, thereby overcoming the traditional tradeoff between actuation speed and force in hydrogel actuators. (Scale bar: 2 cm) Adapted with permission from Reference 3. © 2022 AAAS. (b) Liposomes, spherical vesicles composed of phospholipid bilayers, capable of osmosis due to their inherent structure. (c) "Osmotic engine model" employed in liposome-based actuators within microchannels. Adapted with permission from Reference 90. © 2014 Elsevier.

geometry and elasticity of their structures. The hydraulic cellular processes induce local stress and strain, which is enough to give rise to snap-through instability of the entire plant organ. Although efforts to mimic these rapid plant movements in artificial soft actuators have been made,[84,85] they face persistent challenges—ranging from intricate manufacturing processes and confined movement capacities to the lack of autonomous technologies permitting reversible mode transitions. These challenges emphasize the importance of understanding plant mechanics in-depth and effectively incorporating them into the next generation of bioinspired soft actuators.

In summary, osmotic actuators, despite their evident potential in myriad applications, have their own set of challenges. Continued interdisciplinary research and innovation will be paramount in overcoming these challenges and unlocking the full potential of these actuators in various fields.

Hygroscopic actuation

Hygroscopic actuation in plants

Plant structures, including those composed of dead cells and tissues can display remarkable movements driven by not only metabolic energy, but also the ambient moisture from their surroundings, the latter phenomenon referred to as hygroscopic actuation. This process leverages the hygro-responsive characteristics of plant tissues, specifically their cellulosic components. Changes in ambient humidity can trigger the swelling or shrinking of these tissues, causing various deformations and motions.

The actuation does not rely on turgor pressure, unlike osmotic-based actuations in living cells that involve various dissolved substances. Instead, it is the diffusion of water molecules caused by the humidity difference between tissue and the atmosphere that drives these movements. Water molecules diffusing into dry tissue get trapped within hydrophilic groups present in the cell walls, leading to tissue deformation. Hygroscopic actuation does not require a complex structure nor the use of metabolic energy, yet it operates effectively across a broad range of humidity levels.

It has been instrumental in the survival and propagation strategies of various plant species. For instance, the family of *Aizoaceae*, known as ice plants, use protective valves that mechanically open only when they are sufficiently hydrated by water on their seed capsules to survive and propagate in arid habitats.[91] The resurrection plant (*Selaginella lepidophylla*) shown in **Figure 5**a can survive completely dried for several years, while its stems are compactly curled to form a spherical nest-ball shape to protect inner stems. Once hydrated, they gradually uncurl as programmed and the inner stem can start photosynthesis again.[92]

Plants demonstrate various deformation modes due to hygroscopic actuation, including bending, helical coiling, and twisting, all of which can be achieved with a relatively simple structure. For instance, pine cones use hygroscopic actuation to bend their scales and disperse seeds when the atmosphere becomes dry (Figure 5b). Certain seeds, such as those from wild wheat,[93] *Pelargonium*,[94,95] and *Erodium*,[96] use hygroscopic actuation to bury themselves in soil either by bending or helical coiling their long appendages called awns, thereby creating favorable conditions for germination (Figure 5c–d).

Mechanics of hygroscopic-induced deformations in plants

The hygroscopic motions, including bending, helical coiling, and twisting in plant tissues occur due to the hygroscopically active layer in the tissues. The tissue that generates this movement typically consists of multiple layers of cells whose walls are wrapped with microfibrils. When tissue is exposed to variation of surrounding humidity, the cell walls containing hygro-expansive substances such as pectin and amorphous cellulose expand perpendicular to the orientation of the inextensible fibril, which is key to programming the deformation mode, including bending, helical coiling, and twisting.[19] These actuations are usually realized by a simple bilayer structure combining a hygroscopically active layer with an inactive layer. Due to the difference in hygroscopic expansion ratio and flexural rigidity between the combined layers, the bilayer changes its curvature when the surrounding humidity varies. One of the primary reasons plants utilize these structures to create movement is because they can maximize the amount of deformation with minimal resources. Despite its simple structure, the actuation distance achieved by bending is much greater than by swelling of hygroscopic material itself. For instance, when a bilayered scale of the pine cone with a length of 20 mm experiences an 80% change in humidity, the tip of the scale can move approximately 20 mm, while the hygroscopic layer, which is several hundred micrometers thick, expands only by 3–4% or a few micrometers compared to its original dry length.[97]

The amount of bending actuation caused by a change in humidity can be predicted through the hygroscopic stress generated by the gradient of hygroscopic strain in the active layer. The hygroscopic strain distribution can be obtained by solving the diffusion equation of moisture. As surrounding humidity changes, water molecules diffuse into the active layer and humidity level inside the layer over time, $\phi(z,t)$ follows the diffusion equation, $\partial\phi/\partial t = D_c\partial^2\phi/\partial z^2$, where t is time, D_c is diffusion coefficient, z is the distance from the outermost surface of the active layer, which is set to be the reference plane. The total strain in the active layer is written as $\epsilon(z,t) = \epsilon_0 - \kappa z - \epsilon_h$, where ϵ_0, κ, and ϵ_h are the strain in the reference plane, the bending curvature, and the hygroscopic strain, respectively. The hygroscopic strain, $\epsilon_h = \alpha_h\Delta\phi$ linearly increases with the change in humidity, $\Delta\phi$, where α_h is the hygroscopic swelling coefficient. From the constitutive equation written as $\sigma = E\epsilon$, where σ and E denote local stress and elastic modulus, respectively. The bending force, F and moment, M are obtained by integrating the local stress, $F = \int \sigma dz$ and $M = \int \sigma z dz$. Assuming zero external loads, the theory of laminar composites[98] allows us to

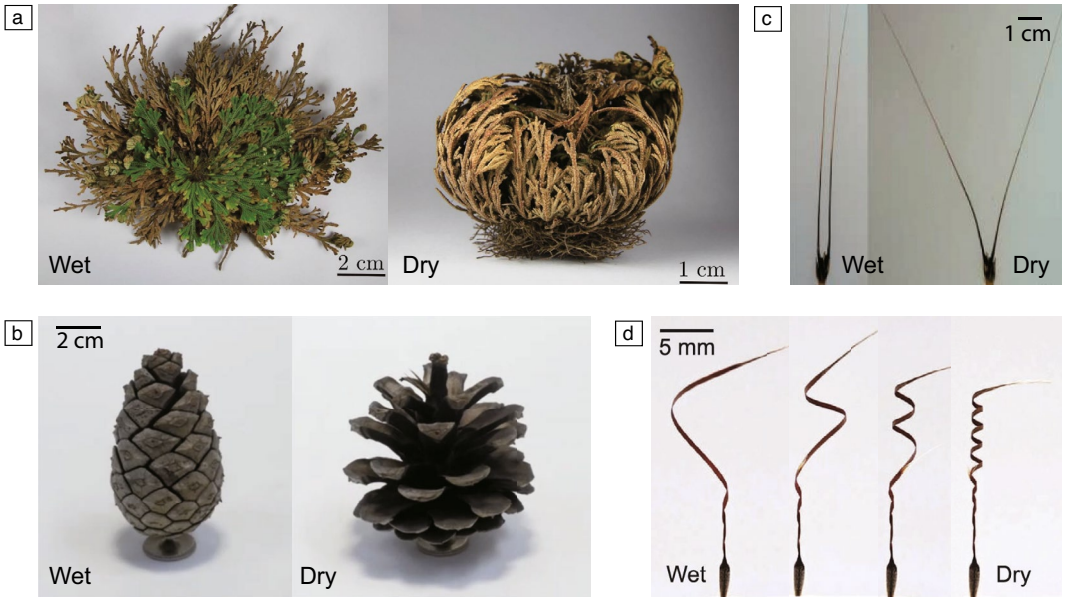

Figure 5. Hygroscopic actuation in plants. (a) Curling and uncurling motion of *Selaginella lepidophylla* known as resurrection plant. Adapted with permission from Reference 92. © 2015 Springer Nature. (b) Scales of pine cone responding to surrounding humidity variation to release its seed under a favorable environmental condition. Seeds of (c) wild wheat and (d) *Pelargonium* have long appendages that can make bending and coiling motion to bury themselves into the soil by repeating bending and coiling motions, respectively. (c) Adapted with permission from Reference 93. © 2007 AAAS. (d) Adapted with permission from Reference 95 with permission. © 2020 Elsevier.

write $F = A\epsilon_0 - B\kappa - F_\alpha = 0$ and $M = B\epsilon_0 - D\kappa - M_\alpha = 0$, where $A = \int E\mathrm{d}z$, $B = \int Ez\mathrm{d}z$, $D = \int Ez^2\mathrm{d}z$, $F_\alpha = \int E\epsilon_h\mathrm{d}z$, and $M_\alpha = \int E\epsilon_h z\mathrm{d}z$. Finally, the curvature is given by $\kappa = (AM_\alpha - BF_\alpha)/B^2 - AD$. As the humidity distribution in the active layer is predicted as a function of time, the consequent temporal change of curvature can be obtained.[99]

The bending deformation of the bilayer actuator having the total thickness, h is simply expressed as $\kappa = \alpha_h \Delta\phi f(m,n)h^{-1}$ with $f(m,n) = 6(1+m)^2/\left[3(1+m)^2 + (1+mn)\left(m^2 + 1/mn\right)\right]$, where m and n, respectively, represent the ratios of the active to inactive layers' thickness and elastic modulus.[100] There is an optimal combination of the thickness for given layer materials to generate maximum deformation. But the optimal design to maximize the bending does not guarantee the maximum speed of motion. The time required for the active layer to be fully saturated, $t_s = h_a^2/D_c$ with h_a being the thickness of active layer and D_c the vapor diffusivity, increases with the thicker active layer, meaning that thick actuators are disadvantageous in terms of actuation speed despite their strong force.

Our physical model reveals that to find the seed awn of wild wheat needs over 100 s to become fully saturated. It has active and inactive layers of thicknesses of approximately 200 μm and 400 μm, respectively, with high elastic moduli of 10–20 GPa. This design is close to the thickness combination resulting in maximum deformation when calculated based on the materials properties of the seed awn. Thus, wild wheat can generate enough energy to bury its seeds into soil, but its bending speed is quite low. As wild wheat generates motion by harnessing energy from the humidity changes between day and night, the seed is speculated to have found the optimal balance between actuation force and response time to make the most efficient use of these humidity changes.

The hygroscopic actuation of plants allows for various adjustments in deformation modes, output, and operating speed by making simple design changes in their simple structures. Therefore, many attempts are being made to demonstrate artificial actuators that mimic the movements of plants with such advantages. In the following, we will introduce various hygroscopic actuators made from natural materials as well as synthetically produced polymers.

Hygroscopic bending actuators

One of the initial attempts to create an actuator inspired by the hygroscopic movement of plants is a bilayer structure comprising paper and a polymer sheet as shown in **Figure 6**a.[100] Paper, a compressed stack of cellulose fibers,[101,102] is one of the most common hygroexpansive materials. As noted in **Table I**, not only the paper, but various materials from nature such as processed wood[5,103] and Bacillus spore[104] and artificially synthesized ones such as liquid crystal,[105,106] graphene oxide,[107,108] and hygroscopic polymers[95,109–115] have been utilized for building hygroscopic bending actuators as fabricated via spin coating,[116] drop casting,[104] or dip coating.[109]

In general, the diffusion coefficients of hygroscopic materials are similar, being on the order of approximately 10^{-12} $m^2\ s^{-1}$. To achieve a rapid response, the diffusion coefficient

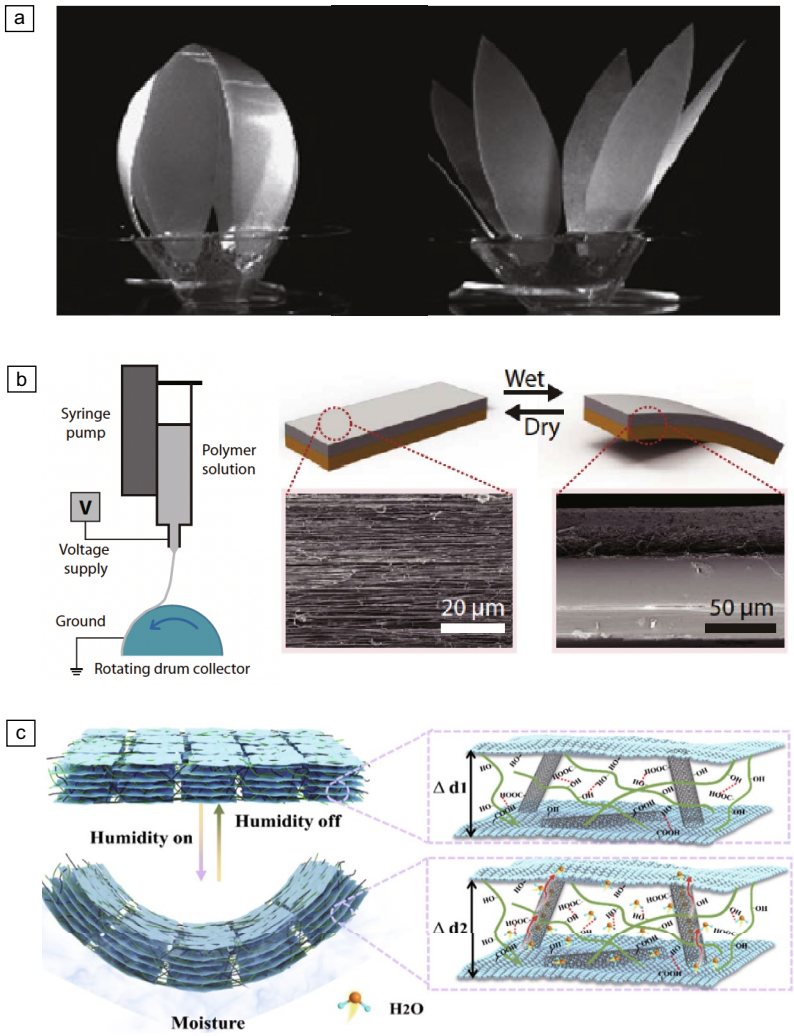

Figure 6. Examples of hygroscopic bending actuators. (a) The bilayer actuator consisting of polymer sheet and paper. Adapted with permission from Reference 100. © 2009 The Royal Society. (b) Directional electrospinning of polymer solution yields the active layer with porous structure consisting of aligned nanofibers, which enables the fast response. Adapted with permission from Reference 8. © 2018 AAAS. (c) A composite layer made up of celullose nanofibers/carbon nanotubes/graphene oxide via vacuum-assisted self-assembly method has a porous structure having numerous nanochannels, which enables the fast transportation of water molecules. Adapted with permission from Reference 107. © 2021 American Chemical Society.

of the hygroscopic materials should be improved by adopting various processes. Shin et al.[8] formed a porous layer by stacking electrospun poly(ethylene oxide) (PEO) nanofibers (Figure 6b). As water molecules can travel more freely inside the porous layer than dense solids, the effective diffusivity of the layer can increase to ~10^{-10} m^2 s^{-1}. Furthermore, to increase the responsivity, one can adopt a composite layer structure having high surface area-to-volume ratio. Wei et al.[107] fabricated a composite layer consisting of cellulose nanofibers (CNFs), carbon nanotubes (CNTs), and graphene oxide (GO) via a vacuum-assisted self-assembly process. Owing to the superior sensitivity to moisture response of CNFs and GO, the actuator rapidly responds to humidity change (Figure 6c). Also, the porous structure with numerous nanochannels formed during the self-assembly process accelerates the transportation of water molecules through the sheet. Through these methods, it was possible to achieve a fast response speed of thick actuators.

The bending actuators can power soft robots, which move forward with the aid of ratchets rectifying the movement in one direction.[8,109] They have been used in soft grippers that deform to grab objects[106] and a cloth maintaining constant humidity level in its interior.[117] Moreover, bending actuators made of wood can be applied to building exteriors, enabling them to interact with the surrounding environment.[118–121]

Helical coiling and twisting actuators

Among hygroscopic deformations exhibited by plants, helical coiling and twisting movements can generate rotation of thin strip-shaped structures such as seed awns as shown in Figure 5d. Such rotation enables the seeds to penetrate soft materials such as soil with lower drag.[94,96] In the bilayer configuration consisting of hygroscopically active and inactive layers, the cell walls in the active layer are constrained by cellulose microfibrils in a tilted helix. Individual cylindrical cells helically coil when dried, leading to collective coiling deformation of the bilayer. The tilted helices winding up the cell walls in the active layer can be approximated as aligned inextensible fibrils that guide the swelling of extensible matter only in the direction parallel to the fibrils, as depicted in **Figure 7**a. Employing a similar approach, multiple techniques for adjusting the expansion direction have been implemented to attain helical coiling or twisting motions.

Abraham et al.[122] implemented coiling by wrapping a sponge with a thread so that the thread would restrict expansion as shown in Figure 7b. Erb et al.[113] showed that it is possible to control the direction of expansion through partial reinforcement as alumina particles in the uncured hydrogel were aligned under the magnetic field, while the hydrogel cures. By irradiating UV light on a shape-memory polymer sheet, the degree of moisture absorption can be partially varied by allowing Fe^{3+} ions to exchange electrons with the polymer (Figure 7c).[114] This method enables the control of the desired deformation in specific areas. Such actuators are not only

Table I. Examples of artificial hygroscopic actuators made up of natural and artificial materials.

Type	Mode of Deformation	Active Layer	Inactive Layer	Directionality Control	References
Natural materials	Bending	Paper	Polymer sheet	–	100
		Bacillus spores	Latex sheet	–	104
		Escherichia coli	Latex	Microprinting	117
	Bending/Coiling	Sponge	Thread	Sewing thread to confine the expansion	122
		Fused granular fabricated wood	–	3D printed stiffness gradient	103
		Processed wood	–	Molding	5
Artificially synthesized materials	Bending	Poly(acrylic acid)/poly(allylamine hydrochloride)	NOA63	–	109
		Liquid crystal	–	UV light	105
		Poly(allylamine hydrochloride)/poly(acrylic acid)	Poly(tetrafluoroethylene)	-	110
		Pentaerythritol ethoxylate–polypyrrole	–	–	116
		Polydopamine-modified Mxene/bacterial cellulose nanofiber	–	–	111
		Poly(ethylene oxide)	PVDF	–	112
		GO/CNF/CNT	–	–	107
		Cellulose stearoyl ester	–	–	126
		Chitosan/graphene oxide	–	–	127
	Bending/Coiling	Reinforced alumina hydrogel	–	Aligning alumina using magnetic field	113
		Poly(ethylene-*co*-acrylic acid) (EAA)	EAA with Fe_3^+-carboxylate	Photopatterning	114
		Liquid-crystal elastomer with different alignment angles	–	Shear alignment using 3D printing	106
		Poly(ethylene oxide)	Polymer film	Directional electrospinning	95
		Graphene oxide (wavy)	Graphene oxide (smooth)	Grating templates	108

photoprogrammable but also reprogrammable in terms of the deformation patterns.

A slender fiber bundle capable of significant lengthwise expansion is also useful in controlling the deformation direction. Electrospinning of hygroexpansive materials such as PEO (poly(ethylene oxide)) was utilized to create unidirectionally aligned nanofiber bundles, which enforces the active layer to expand in one direction (Figure 7d).[8,95] After combining the nanofiber bundle with a hygroscopically inactive layer to build a bilayer actuator, the helical coiling can be achieved by trimming the bending actuator at a specific angle. Additionally, grating templates were used to create groove-shaped graphene oxide layers, which expand in the direction of the grooves.[108] Three-dimensional printing of hygroscopic materials such as wood polymer composite[123,124] and liquid crystal are also candidates to realize this scheme. As shown in Figure 7e, liquid crystal is aligned in one direction by shear force during the printing process.[106] More recently, a method that involves 3D printing of fused wood granules to pattern the deformation degree in specific areas was introduced.[103]

Limitations and perspectives of hygroscopic actuators

Various artificial actuators harnessing environmental humidity have been demonstrated by mimicking the hygroscopic actuation of plants. However, the application of these actuators is limited to simple reciprocating motions, as can be seen in locomotion of soft robots.[5,8,108,109] For further application of artificial hygroscopic actuators, the following limitations of current hygroactuation technology need to be overcome: (1) The actuation is based on thin-plate shapes, resulting in relatively small force and energy; (2) the frequency of motion is passively determined by the humidity variation around the actuator; (3) deformation modes of hygroscopic actuation, including bending, helical coiling, and twisting, differ from those of traditional mechanical actuators such as heat engines and motors, complicating the operation of existing machines; and (4) there is a lack of research on the durability of actuators to ensure their repetitive movements.

In terms of the energy generated by the bending deformation of the actuator, there is a tradeoff between the operation speed and output energy. For instance, a thicker layer can produce greater energy, but the response time increases proportional to the square of the thickness. To obtain a stronger output without sacrificing the operation speed, Luo et al.[5] attached multiple awns to a soft robot that moves like a self-burrowing seed. Chen et al.[125] did not only increase the magnitude of energy by connecting actuators in a repeated zigzag pattern and connecting multiple bundles in parallel, but also created

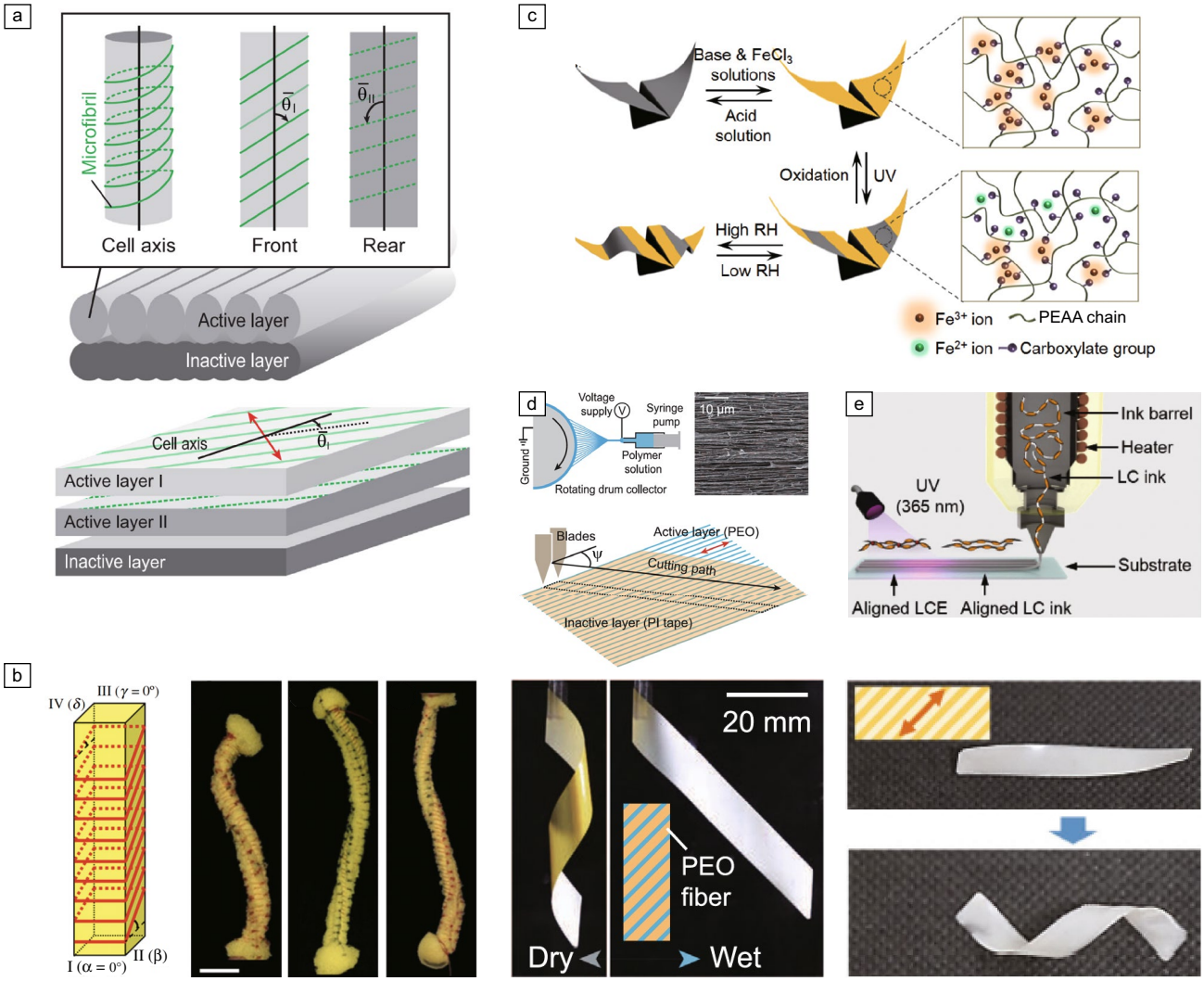

Figure 7. Fabrication methods of coiling and twisting actuators. (a) Schematics of the bilayer structure of the awn. The cell walls in the active layer are constrained by cellulose microfibrils in a tilted helix. Due to the constraint, the cell expands perpendicular to the microfibril indicated in the red arrow. Adapted with permission from Reference 95. © 2020 Elsevier. (b) Wrapping a sponge with a thread that acts as a mechanical constraint. Depending on the orientation of the thread, the pitch and radius of coiling motion change. (Scale bar: 2 cm) Adapted with permission from Reference 122. © 2012 The Royal Society. (c) Controlling the deformation of a shape-memory polymer sheet by UV irradiation to create spatial patterns of the expansion rate to relative humidity (RH). Adapted with permission from Reference 114. © 2022 American Chemical Society. (d) Implementing a coiling actuator by cutting a unidirectionally deposited nanofiber mesh to form a specific angle with the direction of the fiber arrangement. Adapted with permission from Reference 95. © 2020 Elsevier. (e) During the 3D printing process of liquid-crystal elastomer (LCE), the LC is aligned by the shear force. The LC-based actuator shows helical coiling motion. Adapted with permission from Reference 106. © 2021 Wiley.

linear motion through bending deformation (**Figure 8**a). Using a chamber that opens and closes the window according to the interior humidity level, the frequency of the actuation can be controlled, as shown in Figure 8b–c. Using a humidity-controlled chamber, one can rotate a shaft inside, which is connected to a wheel of a vehicle, so that humidity variation drives a car (Figure 8c).[9] These endeavors suggest the possibility of the hygroscopic actuators replacing the conventional actuation systems of common machines.

Moreover, the performance and durability of actuators comprising bilayer structures are critical factors to consider for their long-term use in various applications. However, limited research exists on the possible decrease in durability and degradation of performance due to repetitive movements in such actuators. A deeper understanding of the damage to materials composing each layer, as well as the deformation at the interface between the hygroscopically active and inactive layers, can provide essential insights for designing structures and materials with improved durability. Under repeated operation of the actuator, the stress is inevitably concentrated at the interface where the two different materials comprising the bilayer are joined, potentially leading to a decline in the performance of the actuator. One potential solution to improve durability regarding the interface is adding a layer

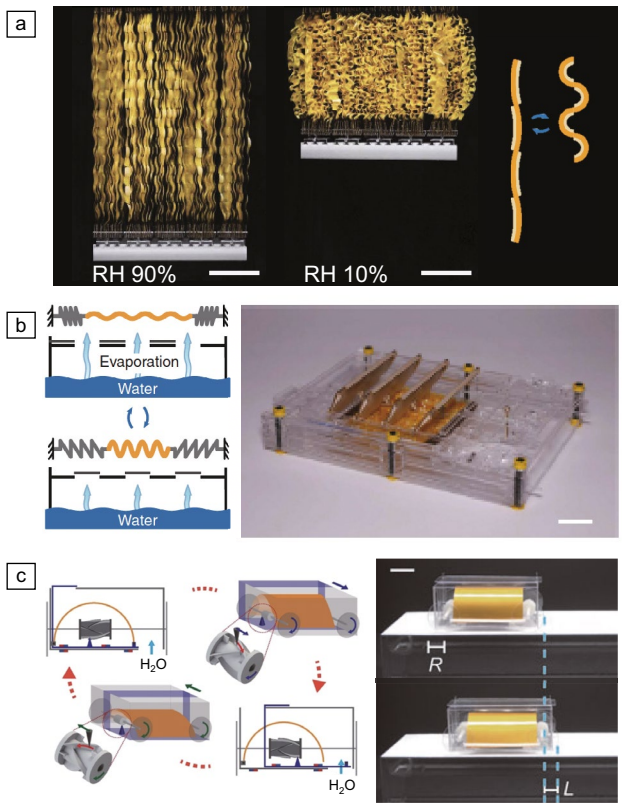

Figure 8. Strategies for the universal use of hygroscopic actuators in conventional machines. (a) Scaling up the bending actuator by connecting multiple actuator units in parallel. The actuator unit consists of bending actuators in a zigzag pattern.[125] (Scale bar: 1 cm) RH, relative humidity. (b) A chamber having a window, which is connected to the actuator, opens and closes depending on the humidity level inside the chamber. (Scale bar: 2 cm) Adapted with permission from Reference 125. © 2015 Springer Nature. (c) Schematics of a chamber with a periodically moving window. The shaft rotates as the window of the chamber opens and closes, leading to the rotation of the wheels and locomotion of the vehicle. (Scale bar: 1 cm) Adapted with permission from Reference 9. © 2023 Mary Ann Liebert Inc.

that minimizes the deformation imbalance between the active and inactive layers such as a layer with negative Poisson's ratio or gradually changing expansion ratio. This modification could distribute strain more evenly and minimize deformation at the interface, ultimately enhancing durability. Furthermore, the performance of hygroscopic actuators could degrade due to hysteresis occurring as water molecules accumulate inside hygroscopic materials during the absorption and release processes. A remedy can come from developing materials that can efficiently absorb and release water molecules quickly, even with repeated usage.

Conclusion

We have introduced the physical principles of osmotic and hygroscopic actuation, which allow plants to create movement using only water transportation. We have also reviewed the latest trends in artificial actuators that utilize these principles.

Plant-inspired actuators have made significant strides and demonstrated impressive progress in utilizing water as a power source. This is mainly thanks to the understanding of the principles behind plant movement and the advancements in materials and processing technologies. Many attempts have been made to achieve complicated motion including locomotion, rotation, and shape morphing based on plants' motile strategies.

However, challenges remain in applying plant-inspired actuation to soft sensors, actuators, robots, and other soft machines. One of the central challenges is increasing the speed and output power of actuation to a level comparable to other actuators. Both osmotic and hygroscopic actuations have a tradeoff between speed and output power, requiring a balanced approach to improving performance as needed. Furthermore, while plants can achieve complex movements through intricate internal structure and mechanisms, the deformation modes created by our current soft actuators are generally simpler, so that methods to generate more complex movements await to be explored.

In conclusion, the principles and strategies for motility in the plant kingdom inspire not just the development of efficient actuation systems but also the creation of smart devices capable of sensitive environmental interaction. The potential for this research to revolutionize and miniaturize intelligent control systems is vast and largely untapped, underscoring the need for continued exploration and innovation.

Acknowledgments

This work was supported by the National Research Foundation of Korea (Grant Nos. 2018-052541 and 2021-017476) and the Gachon University research fund of 2019 (GCU-2019-0800). The administrative support from SNU Institute of Engineering Research is acknowledged.

Author contributions

B.S. and S.J. conducted literature review. B.S., S.J., and M.C. wrote the initial draft. K.P. and H.-Y.K. conceived the project and supervised the article.

Data availability

Data sharing not applicable to this article as no data sets were generated or analyzed during the current study.

Conflict of interest

On behalf of all authors, the corresponding author states that there is no conflict of interest.

References

1. P. Chen, Y. Xu, S. He, X. Sun, S. Pan, J. Deng, D. Chen, H. Peng, *Nat. Nanotechnol.* **10**, 1077 (2015)
2. R. Geer, S. Iannucci, S. Li, *Front. Robot. AI* **7**, 17 (2020)
3. H. Na, Y.-W. Kang, C.S. Park, S. Jung, H.-Y. Kim, J.-Y. Sun, *Science* **376**, 301 (2022)
4. F. Zhang, M. Yang, X. Xu, X. Liu, H. Liu, L. Jiang, S. Wang, *Nat. Mater.* **21**, 1357 (2022)

5. D. Luo, A. Maheshwari, A. Danielescu, J. Li, Y. Yang, Y. Tao, L. Sun, D.K. Patel, G. Wang, S. Yang, T. Zhang, L. Yao, *Nature* **614**, 463 (2023)
6. C.J. Park, J. Ha, H.-R. Lee, K. Park, J.-Y. Sun, H.-Y. Kim, *Proc. Natl. Acad. Sci. U.S.A.* **120**, e2211416120 (2023)
7. I. Must, E. Sinibaldi, B. Mazzolai, *Nat. Commun.* **10**, 344 (2019)
8. B. Shin, J. Ha, M. Lee, K. Park, G.H. Park, T.H. Choi, K.-J. Cho, H.-Y. Kim, *Sci. Robot.* **3**, eaar2629 (2018)
9. M. Choi, B. Shin, H.-Y. Kim, *Soft Robot.* **10**, 1171 (2023)
10. E.W. Hawkes, L.H. Blumenschein, J.D. Greer, A.M. Okamura, *Sci. Robot.* **2**, eaan3028 (2017)
11. I. Fiorello, F. Meder, A. Mondini, E. Sinibaldi, C. Filippeschi, O. Tricinci, B. Mazzolai, *Commun. Mater.* **2**, 103 (2021)
12. S.N. Gorb, *Philos. Trans. A Math. Phys. Eng. Sci.* **366**(1870), 1557 (2008)
13. Y. Qi, C. Zhou, Y. Qiu, X. Cao, W. Niu, S. Wu, Y. Zheng, W. Ma, H. Ye, S. Zhang, *Mater. Horiz.* **9**, 1243 (2022)
14. Y. Pan, Z. Yang, C. Li, S.U. Hassan, H.C. Shum, *Sci. Adv.* **8**, eabo1719 (2022)
15. Y. Jung, K. Park, K.H. Jensen, W. Kim, H.-Y. Kim, *J. R. Soc. Interface* **16**, 20190556 (2019)
16. N.E. Robbins, J.R. Dinneny, *Proc. Natl. Acad. Sci. U.S.A.* **115**, E822 (2018)
17. L.X. Dupuy, M. Mimault, D. Patko, V. Ladmiral, B. Ameduri, M.P. MacDonald, M. Ptashnyk, *Curr. Opin. Genet. Dev.* **51**, 18 (2018)
18. K.H. Jensen, K. Berg-Sørensen, H. Bruus, N.M. Holbrook, J. Liesche, A. Schulz, M.A. Zwieniecki, T. Bohr, *Rev. Mod. Phys.* **88**, 035007 (2016)
19. J. Dumais, Y. Forterre, *Annu. Rev. Fluid Mech.* **44**, 453 (2012)
20. Y. Forterre, *J. Exp. Bot.* **64**, 4745 (2013)
21. Q. Guo, E. Dai, X. Han, S. Xie, E. Chao, Z. Chen, *J. R. Soc. Interface* **12**, 20150598 (2015)
22. T. Sibaoka, *Annu. Rev. Plant Physiol.* **20**, 165 (1969)
23. D.J. Cosgrove, *Nat. Rev. Mol. Cell Biol.* **6**, 850 (2005)
24. E. Münch, *Die Stoffbewegungen in der Pflanze* (G. Fischer, Jena, 1930)
25. K.H. Jensen, J. Liesche, T. Bohr, A. Schulz, *Plant Cell Environ.* **35**, 1065 (2012)
26. T. Kanahama, S. Tsugawa, M. Sato, *Sci. Rep.* **13**, 2063 (2023)
27. A. Kempe, T. Lautenschläger, A. Lange, C. Neinhuis, *Plant Biol.* **16**(1), 264 (2014)
28. K.J. Niklas, *Am. J. Bot.* **76**, 929 (1989)
29. A.K. Bastola, P. Soffiatti, M. Behl, A. Lendlein, N.P. Rowe, *J. R. Soc. Interface* **18**, 20210040 (2021)
30. H. Meidner, T.A. Mansfield, *Physiology of Stomata* (McGraw-Hill, London, 1968)
31. T. Kinoshita, Y. Hayashi, *Int. Rev. Cell Mol. Biol.* **289**, 89 (2011)
32. J.I. Schroeder, R. Hedrich, J.M. Fernandez, *Nature* **312**, 361 (1984)
33. K. Kameyama, Y. Kishi, M. Yoshimura, N. Kanzawa, M. Sameshima, T. Tsuchiya, *Nature* **407**, 37 (2000)
34. A.G. Volkov, J.C. Foster, K.D. Baker, V.S. Markin, *Plant Signal. Behav.* **5**(10), 1211 (2010)
35. H.W.J. Ragetli, M. Weintraub, E. Lo, *Can. J. Bot.* **50**, 159 (1972)
36. S.E. Williams, B.G. Pickard, *Planta* **103**, 193 (1972)
37. S.E. Williams, B.G. Pickard, *Planta* **103**, 222 (1972)
38. M. Weintraub, *New Phytol.* **50**(3), 357 (1952)
39. M. Malone, *New Phytol.* **128**(1), 49 (1994)
40. H. Stoeckel, K. Takeda, *J. Membr. Biol.* **146**, 201 (1995)
41. Y. Forterre, J.M. Skotheim, J. Dumais, L. Mahadevan, *Nature* **433**, 421 (2005)
42. J.R. Di Palma, R. Mohl, W. Best, *Science* **133**, 878 (1961)
43. G.M. Durak, T. Speck, S. Poppinga, *Front. Plant Sci.* **13**, 970320 (2022)
44. G.M. Durak, R. Thierer, R. Sachse, M. Bischoff, T. Speck, S. Poppinga, *Adv. Sci.* **9**, 2201362 (2022)
45. R. Sachse, A. Westermeier, M. Mylo, J. Nadasdi, M. Bischoff, T. Speck, S. Poppinga, *Proc. Natl. Acad. Sci. U.S.A.* **117**, 16035 (2020)
46. P. Simons, *The Action Plant* (Blackwell Publishing, Oxford, 1992)
47. F. Lloyd, *The Carnivorous Plants* (Donald Publishing, Hampton Falls, 1942)
48. G. Joos, I.M. Freeman, *Theoretical Physics* (Courier Corporation, North Chelmsford, 2013)
49. P. Atkins, P.W. Atkins, J. de Paula, *Atkins' Physical Chemistry* (Oxford University Press, Oxford, 2014)
50. P. Bharmoria, H. Gupta, V. Mohandas, P.K. Ghosh, A. Kumar, *J. Phys. Chem. B* **116**, 11712 (2012)
51. N.J.W. Clipson, A.D. Tomos, T.J. Flowers, R.G.W. Jones, *Planta* **165**, 392 (1985)
52. Y.X. Kim, B. Stumpf, J. Sung, S.J. Lee, *Cells* **7**(10), 180 (2018)
53. H. Schneider, J. Zhu, U. Zimmermann, *Plant Cell Environ.* **20**, 221 (1997)
54. K. Itoh, Y. Nakamura, H. Kawata, T. Yamada, E. Ohta, M. Sakata, *Plant Cell Physiol.* **28**, 987 (1987)
55. P.J. Franks, T.N. Buckley, J.C. Shope, K.A. Mott, *Plant Physiol.* **125**, 1577 (2001)
56. H.L. Gorton, *Plant Physiol.* **83**, 945 (1987)
57. H.L. Gorton, *Plant Physiol.* **83**, 951 (1987)
58. H.-X. Chang, L.A. Miller, G.L. Hartman, *Phytopathology* **104**, 977 (2014)
59. O. Kedem, A. Katchalsky, *Biochim. Biophys. Acta* **27**, 229 (1958)
60. K.S. Spiegler, O. Kedem, *Desalination* **1**, 311 (1966)
61. E. Steudle, "Water Flow in Plants and Its Coupling to Other Processes: An Overview," in *Methods in Enzymology* (Academic, New York, 1989), p.183
62. E. Sinibaldi, A. Argiolas, G.L. Puleo, B. Mazzolai, *PLoS ONE* **9**, e102461 (2014)
63. E. Sinibaldi, G. Puleo, F. Mattioli, V. Mattoli, F. Di Michele, L. Beccai, F. Tramacere, S. Mancuso, B. Mazzolai, *Bioinspir. Biomim.* **8**, 025002 (2013)
64. S. Yu-Chuan, L. Liwei, A.P. Pisano, *J. Microelectromech. Syst.* **11**, 736 (2002)
65. E. Freeman, L. Weiland, *J. Intell. Mater. Syst. Struct.* **23**, 1395 (2012)
66. K. Dušek, D. Patterson, *J. Polym. Sci.* **6**, 1209 (1968)
67. T. Tanaka, *Phys. Rev. Lett.* **40**, 820 (1978)
68. Q. Xing, K. Yates, C. Vogt, Z. Qian, M.C. Frost, F. Zhao, *Sci. Rep.* **4**, 4706 (2014)
69. H. Holback, Y. Yeo, K. Park, "Hydrogel Swelling Behavior and Its Biomedical Applications," in *Biomedical Hydrogels* (Elsevier, Amsterdam, 2011), p. 3
70. S.Y. Yang, E.D. O'Cearbhaill, G.C. Sisk, K.M. Park, W.K. Cho, M. Villiger, B.E. Bouma, B. Pomahac, J.M. Karp, *Nat. Commun.* **4**, 1702 (2013)
71. A.K. Bastola, N. Rodriguez, M. Behl, P. Soffiatti, N.P. Rowe, A. Lendlein, *Mater. Des.* **202**, 109515 (2021)
72. D.J. Beebe, J.S. Moore, J.M. Bauer, Q. Yu, R.H. Liu, C. Devadoss, B.-H. Jo, *Nature* **404**, 588 (2000)
73. A. Shastri, L.M. McGregor, Y. Liu, V. Harris, H. Nan, M. Mujica, Y. Vasquez, A. Bhattacharya, Y. Ma, M. Aizenberg, O. Kuksenok, A.C. Balazs, J. Aizenberg, X. He, *Nat. Chem.* **7**, 447 (2015)
74. L. Dong, A.K. Agarwal, D.J. Beebe, H. Jiang, *Nature* **442**, 551 (2006)
75. A. Nojoomi, H. Arslan, K. Lee, K. Yum, *Nat. Commun.* **9**, 3705 (2018)
76. J. Kim, J.A. Hanna, M. Byun, C.D. Santangelo, R.C. Hayward, *Science* **335**, 1201 (2012)
77. E. Palleau, D. Morales, M.D. Dickey, O.D. Velev, *Nat. Commun.* **4**, 2257 (2013)
78. J.C. Athas, C.P. Nguyen, B.C. Zarket, A. Gargava, Z. Nie, S.R. Raghavan, *ACS Appl. Mater. Interfaces* **8**, 19066 (2016)
79. A. Sydney Gladman, E.A. Matsumoto, R.G. Nuzzo, L. Mahadevan, J.A. Lewis, *Nat. Mater.* **15**, 413 (2016)
80. Y.S. Kim, M. Liu, Y. Ishida, Y. Ebina, M. Osada, T. Sasaki, T. Hikima, M. Takata, T. Aida, *Nat. Mater.* **14**, 1002 (2015)
81. X. Liu, C. Steiger, S. Lin, G.A. Parada, J. Liu, H.F. Chan, H. Yuk, N.V. Phan, J. Collins, S. Tamang, G. Traverso, X. Zhao, *Nat. Commun.* **10**, 493 (2019)
82. R. Yoshida, K. Uchida, Y. Kaneko, K. Sakai, A. Kikuchi, Y. Sakurai, T. Okano, *Nature* **374**, 240 (1995)
83. W. Fan, C. Shan, H. Guo, J. Sang, R. Wang, R. Zheng, K. Sui, Z. Nie, *Sci. Adv.* **5**, eaav7174 (2019)
84. H. Yuk, S. Lin, C. Ma, M. Takaffoli, N.X. Fang, X. Zhao, *Nat. Commun.* **8**, 14230 (2017)
85. Y. Osada, H. Okuzaki, H. Hori, *Nature* **355**, 242 (1992)
86. E. Wang, M.S. Desai, S.-W. Lee, *Nano Lett.* **13**, 2826 (2013)
87. K. Fujiwara, M. Yanagisawa, *ACS Synth. Biol.* **3**, 870 (2014)
88. M. Andes-Koback, C.D. Keating, *J. Am. Chem. Soc.* **133**, 9545 (2011)
89. K. Shoji, R. Kawano, *Lab Chip* **19**, 3472 (2019)
90. K.M. Stroka, H. Jiang, S.-H. Chen, Z. Tong, D. Wirtz, S.X. Sun, K. Konstantopoulos, *Cell* **157**, 611 (2014)
91. M.J. Harrington, K. Razghandi, F. Ditsch, L. Guiducci, M. Rueggeberg, J.W.C. Dunlop, P. Fratzl, C. Neinhuis, I. Burgert, *Nat. Commun.* **2**, 337 (2011)
92. A. Rafsanjani, V. Brulé, T.L. Western, D. Pasini, *Sci. Rep.* **5**, 8064 (2015)
93. R. Elbaum, L. Zaltzman, I. Burgert, P. Fratzl, *Science* **316**, 884 (2007)
94. W. Jung, S.M. Choi, W. Kim, H.-Y. Kim, *Phys. Fluids* **29**, 041702 (2017)
95. J. Ha, S.M. Choi, B. Shin, M. Lee, W. Jung, H.-Y. Kim, *Extreme Mech. Lett.* **38**, 100746 (2020)
96. D. Evangelista, S. Hotton, J. Dumais, *J. Exp. Biol.* **214**, 521 (2011)
97. C. Dawson, J.F.V. Vincent, A.-M. Rocca, *Nature* **390**, 668 (1997)
98. Z. Gürdal, R.T. Haftka, P. Hajela, *Design and Optimization of Laminated Composite Materials* (Wiley, New York, 1999)
99. B. Shin, Y. Jung, M. Choi, H.-Y. Kim, *Phys. Rev. Appl.* **18**, 044061 (2022)
100. E. Reyssat, L. Mahadevan, *J. R. Soc. Interface* **6**(39), 951 (2009)
101. M. Lee, S. Kim, H.-Y. Kim, L. Mahadevan, *Phys. Fluids* **28**, 042101 (2016)
102. S. Poppinga, P. Schenck, O. Speck, T. Speck, B. Bruchmann, T. Masselter, *Biomimetics* **6**, 42 (2021)
103. T. Cheng, D. Wood, L. Kiesewetter, E. Özdemir, K. Antorveza, A. Menges, *Bioinspir. Biomim* **16**, 055004 (2021)
104. X. Chen, L. Mahadevan, A. Driks, O. Sahin, *Nat. Nanotechnol.* **9**, 137 (2014)
105. D.J. Broer, C.M.W. Bastiaansen, M.G. Debije, A.P.H.J. Schenning, *Angew. Chem. Int. Ed.* **51**, 7102 (2012)
106. K. Kim, Y. Guo, J. Bae, S. Choi, H.Y. Song, S. Park, K. Hyun, S.-K. Ahn, *Small* **17**, 2100910 (2021)
107. J. Wei, S. Jia, J. Guan, C. Ma, Z. Shao, *ACS Appl. Mater. Interfaces* **13**, 54417 (2021)
108. M. Wang, Q. Li, J. Shi, X. Cao, L. Min, X. Li, L. Zhu, Y. Lv, Z. Qin, X. Chen, K. Pan, *ACS Appl. Mater. Interfaces* **12**, 33104 (2020)
109. Y. Ma, Y. Zhang, B. Wu, W. Sun, Z. Li, J. Sun, *Angew. Chem. Int. Ed.* **50**, 6254 (2011)
110. S.-W. Lee, J.H. Prosser, P.K. Purohit, D. Lee, *ACS Macro Lett.* **2**, 960 (2013)
111. L. Yang, J. Cui, L. Zhang, X. Xu, X. Chen, D. Sun, *Adv. Funct. Mater.* **31**, 2101378 (2021)

112. F. Gong, H. Li, J. Huang, Y. Jing, Z. Hu, D. Xia, Q. Zhou, R. Xiao, *Nano Energy* **91**, 106677 (2022)
113. R.M. Erb, J.S. Sander, R. Grisch, A.R. Studart, *Nat. Commun.* **4**, 1712 (2013)
114. J. Xue, Y. Ge, Z. Liu, Z. Liu, J. Jiang, G. Li, *ACS Appl. Mater. Interfaces* **14**(8), 10836 (2022)
115. L. Cecchini, S. Mariani, M. Ronzan, A. Mondini, N.M. Pugno, B. Mazzolai, *Adv. Sci.* **10**, 2205146 (2023)
116. M. Ma, L. Guo, D.G. Anderson, R. Langer, *Science* **339**, 186 (2013)
117. W. Wang, L. Yao, C.-Y. Cheng, T. Zhang, H. Atsumi, L. Wang, G. Wang, O. Anilionyte, H. Steiner, J. Ou, K. Zhou, C. Wawrousek, K. Petrecca, A.M. Belcher, R. Karnik, X. Zhao, D.I.C. Wang, H. Ishii, *Sci. Adv.* **3**, e1601984 (2017)
118. S. Reichert, A. Menges, D. Correa, *Comput. Aided Des.* **60**, 50 (2015)
119. S. Poppinga, D. Correa, B. Bruchmann, A. Menges, T. Speck, *Integr. Comp. Biol.* **60**, 886 (2020)
120. Y. Tahouni, F. Krüger, S. Poppinga, D. Wood, M. Pfaff, J. Rühe, T. Speck, A. Menges, *Bioinspir. Biomim.* **16**, 055002 (2021)
121. D. Correa, S. Poppinga, M.D. Mylo, A.S. Westermeier, B. Bruchmann, A. Menges, T. Speck, *Philos. Trans. R. Soc. A* **378**, 20190445 (2020)
122. Y. Abraham, C. Tamburu, E. Klein, J.W.C. Dunlop, P. Fratzl, U. Raviv, R. Elbaum, *J. R. Soc. Interface* **9**, 640 (2012)
123. T. Cheng, M. Thielen, S. Poppinga, Y. Tahouni, D. Wood, T. Steinberg, A. Menges, T. Speck, *Adv. Sci.* **8**, 2100411 (2021)
124. E.S. Sahin, T. Cheng, D. Wood, Y. Tahouni, S. Poppinga, M. Thielen, T. Speck, A. Menges, *Biomimetics* **8**, 233 (2023)
125. X. Chen, D. Goodnight, Z. Gao, A.H. Cavusoglu, N. Sabharwal, M. DeLay, A. Driks, O. Sahin, *Nat. Commun.* **6**, 7346 (2015)
126. K. Zhang, A. Geissler, M. Standhardt, S. Mehlhase, M. Gallei, L. Chen, C. Marie Thiele, *Sci. Rep.* **5**, 11011 (2015)
127. Y. Zhang, H. Jiang, F. Li, Y. Xia, Y. Lei, X. Jin, G. Zhang, H. Li, *J. Mater. Chem. A* **5**, 14604 (2017) □

Beomjune Shin is a postdoctoral research fellow at the Georgia Institute of Technology. He earned his BS degree in mechanical engineering from Hanyang University, South Korea, in 2014, followed by a MS degree in 2016 and PhD degree in 2021 in mechanical and aerospace engineering from Seoul National University, South Korea. His current research focuses on exploring the mechanics of soft matter with diverse applications, including soft robots and human–machine interaction. Shin can be reached by email at sbj0602@gmail.com.

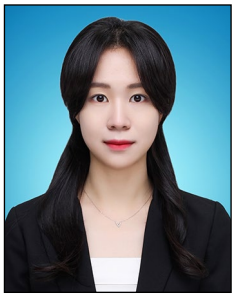

Sohyun Jung is a contract professor in the Department of Mechanical Engineering at Seoul National University, South Korea. She earned her BS degree from Korea University, South Korea, in 2015, and her PhD degree from Seoul National University in 2021. Her research interest revolves around mechanics of microfluids and soft porous media, with applications to bioinspired systems, biomedical devices. Jung can be reached by email at sohyun153@snu.ac.kr.

Munkyeong Choi is a doctoral candidate in the Department of Mechanical Engineering at Seoul National University, South Korea. He specializes in soft robotics, with a focus on projects involving the design of humidity-powered machines that exploit environmental humidity gradients. His innovative research combines expertise in mechanical engineering with a passion for advancing the field of soft robotics. Choi can be reached by email at hungry604@snu.ac.kr.

Keunhwan Park is currently an assistant professor at Gachon University, South Korea, a role he assumed in 2020. Previously, he undertook postdoctoral research at the Technical University of Denmark from 2016 to 2019. He commenced his research journey as a postdoctoral research fellow at Seoul National University, South Korea, from 2015 to 2016. He earned his BSc degree in mechanical and aerospace engineering in 2008, followed by a PhD degree in the same discipline in 2015, both from Seoul National University. His research interests encompass biofluid mechanics and soft-matter physics. Park can be reached by email at kpark@gachon.ac.kr.

Ho-Young Kim is a professor in the Department of Mechanical Engineering at Seoul National University, South Korea. He earned his BS degree from Seoul National University in 1994, and his MS degree in 1996 and PhD in 1999 from the Massachusetts Institute of Technology. He has received several awards, including Seoul National University President's Award for Research Excellence and has been an American Physical Society Fellow since 2017. His research interest revolves around mechanics of microfluids and soft matter, with applications to bioinspired systems, soft machines, and robots. Kim can be reached by email at hyk@snu.ac.kr.